A Thesis Presented to

The Faculty of Alfred University

THE AQUEOUS CORROSION OF NUCLEAR WASTE GLASSES WITH VARYING COMPOSITIONS

Kathryn V. Esham

In Partial Fulfillment of
the Requirements for
The Alfred University Honors Program

May 12, 2014

Under the Supervision of:

Dr. Nathan Mellott, Chair

Dr. Alexis Clare, Committee

Dr. S. K. Sundaram, Committee

ACKNOWLEDGEMENTS

I would like to thank Dr. Nathan Mellott for giving me the opportunity to work with his group, for serving as my honors thesis chair, and for introducing me to the world of research. I'd like to thank Yuxuan Gong for being my mentor throughout the research process, and also for running XPS. Additionally, I'd like to thank Dr. Anthony Wren for use of his lab space, Gerry Wynick for SEM, Dimple Pradhan and Timothy Keenan for ICP, as well as Ana Fredell for running BET endlessly and Eric Teller for help with XRD. Finally, thanks to Dr. Alexis Clare and Dr. S.K. Sundaram for serving on my honors thesis committee.

TABLE OF CONTENTS

LIST OF TABLES iv

LIST OF FIGURES v

ABSTRACT vi

I. HONORS THESIS INTRODUCTION 1

II. EXPERIMENTAL PROCEDURE 6

A. Sample Preparation 6

B. Corrosion Methods 6

C. Materials Characterization 7

III. RESULTS 9

A. X-ray Diffraction 9

B. X-ray Photoelectron Spectroscopy 9

C. Inductively Coupled Plasma Spectroscopy 9

D. Scanning Electron Microscopy 10

IV. DISCUSSION 11

V. CONCLUSIONS 15

VI. FUTURE WORK 16

VII. APPENDIX 17

VIII. REFERENCES 25

LIST OF TABLES

Table 1. Contribution of NBO (a) and resultant NBO/tetrahedron and NBO/BO for each glass composition (b). 17

Table 2. Compositions of Glasses 1, 2, and 3 in (a) mol% and (b) wt%. 17

Table 3. Calculated specific surface area for Glasses 1, 2, and 3 and solution volume satisfying a $10m^{-1}$ ratio. 17

Table 4. Atomic compositions as determined by XPS of (a) Glass 1, (b) Glass 2, and (c) Glass 3, pre-corrosion and after 15-day corrosion. 19

LIST OF FIGURES

Honors Introduction Figures

Figure 1. An example of glass structure containing 4-coordinated formers, modifiers and non-bridging-oxygen. 2

Appendix Figures

Figure 1. XRD patterns of glass powders (a) before and (b) after corrosion.....18

Figure 2. XPS spectra of Glass 1 after 10- and 15-day corrosion in pH=3 and pH=9 solutions. 19

Figure 3. XPS spectra of Glass 2 after 10- and 15-day corrosion in pH=3 and pH=9 solutions. 20

Figure 4. XPS spectra of Glass 3 after 10- and 15-day corrosion in pH=3 and pH=9 solutions. 20

Figure 5. ICP analysis showing release of (a) silicon, (b) sodium, and (c) boron from Glasses 1, 2, and 3 into solutions (•) pH=3 and (◆) pH=9. 21

Figure 6. SEM images captured with SE and BSE at 20,000x magnification of Glass 1 (a) pre-corrosion, and after 15 days in (b) pH=3 and (c) pH=9. 22

Figure 7. SEM images captured with SE and BSE at 20,000x magnification of Glass 2 (a) pre-corrosion, and after 15 days in (b) pH=3 and (c) pH=9. 23

Figure 8. SEM images captured with SE and BSE at 5,000x magnification of Glass 3 (a) pre-corrosion, and after 15 days in (b) pH=3 and (c) pH=9. 24

ABSTRACT

Nuclear energy makes up a significant portion of today's energy industry, unfortunately the by-products are radioactive and need to be safely contained. Glass is currently being considered for use in such a containment unit. In this study, three alumino-borosilicate glasses with varying amounts of Na, Ca, and Zr were mixed to achieve different non-bridging oxygen (NBO) concentrations. The expectation is that the glass with the most NBOs will corrode the fastest, while the glass with the fewest NBOs will corrode the slowest. The glass powders were subjected to 1, 3, 5, 10 and 15 day corrosion periods, in pH 3 and pH 9 solutions, at 90°C. To evaluate the corrosion of each glass, inductively coupled plasma spectroscopy (ICP) was used to measure the amount of ions released into solution, and x-ray photoelectron spectroscopy (XPS) and scanning electron microscopy (SEM) allowed for chemical and visual surface analysis of the glass powders before and after corrosion. XPS and ICP analysis showed leaching in all glasses, possibly indicating the presence of a sodium-boron rich phase. SEM revealed surface feature formation on Glasses 2 and 3. It was determined that glass composition with respect to NBO concentration and testing conditions affected the corrosion of the glasses.

I. HONORS THESIS INTRODUCTION

Nuclear energy makes up a significant portion of the global energy market. Unfortunately, the by-products are dangerous materials containing radionuclides. Methods for recycling the waste by separating out unused elements have been explored. Additionally, efforts to decrease the amount of nuclear waste produced have been successful. Today fossil fuel sources create more waste than nuclear energy[1]. However, there are still significant amounts of nuclear waste that need to be dealt with safely. Glass has been studied as a possible long-term solution for nuclear waste storage.

Nuclear waste immobilization in glasses is done in two general methods: incorporation into the glass structure or encapsulation by the glass. Incorporation into the structure involves adding waste into the glass melt to produce an inhomogeneous glass. Encapsulation involves adding waste materials that are too large to fit into the glass network into the melt to produce a glass containing insoluble compounds[1]. This means that the nuclear waste is added to the raw glass materials, and the combination is melted together to produce a glass that contains the nuclear waste inside. Some of the wastes are small enough that they fit into the glass structure nicely, others are large and need the glass to contain them but not incorporate them. The glass structure is what allows the waste to be contained, and modifying the structure can lead to more effective storage.

In order to properly store nuclear waste a glass needs to have an open structure, allowing for incorporation of the radionuclides. This can be accomplished by forming non-bridging oxygen through the introduction of glass modifiers. Non-bridging oxygen (NBO) are oxygen in the glass structure that are bonded to one network former, such as silicon, boron or possibly aluminum, and have one dangling bond. In contrast, bridging oxygen are bonded to two network formers. When a modifier, such as an alkaline or alkaline earth oxide (Na_2O, CaO, MgO, etc.) is added the bridging oxygen are transformed in NBO. This is demonstrated in the following equation:

$$\mathrm{Si-O-Si} + \mathrm{R_2O} \rightarrow \mathrm{Si-O^-\ R^+} + \mathrm{R^{\pm}O-Si}$$

The figure on the following page illustrates the opening of the structure due to the formation of NBOs.

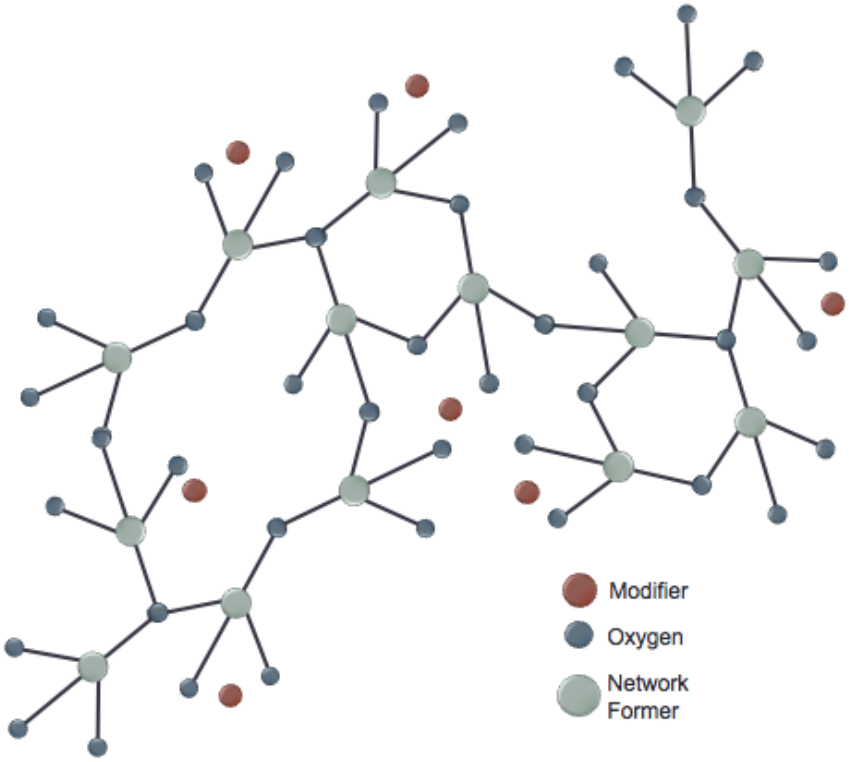

Figure 1. An example of glass structure containing 4-coordinated formers, modifiers and non-bridging-oxygen.

Thus, adding more glass modifiers to the composition creates more NBOs. It might seem that the solution to nuclear waste storage would be to add enough modifiers to open the structure significantly, allowing all wastes to be incorporated. However, the change in structure with the formation of NBOs has a significant effect on the glass properties.

In addition to good storage potential, the glass also needs to have long-term chemically durable to prevent the release of these radionuclides over time. Because a more open structure generally means a weaker network and less chemical durability, it is important to understand the relationship between composition and chemical durability. Since the glasses need to store nuclear waste for the foreseeable future, several long-term studies have been preformed to better understand how the chemical durability of glass changes over time[2-7].

The chemical durability of glass makes it an attractive material for storing nuclear waste. This strength comes from the bonds, like Si-O-Si bonds in silicate glasses. However, silicate glasses have high processing temperatures and tight, closed structures, which would not allow for incorporation of radionuclides. Because of this, most glasses used for this purpose will be borosilicate with some modifiers. The boron breaks up silicon-oxide network, reducing melt temperature while increasing chemical durability. Other additives make the glass processing less expensive and also change the properties. Nuclear waster storage borosilicates often contain aluminum and several alkali and alkaline earth oxide modifiers. While the exact structure of these alumino-borosilicate glasses is currently unknown, it is worth noting the impact of modifiers in other systems to understand how they will affect the properties of the nuclear waste storage glass.

Silicon and boron are both network formers in borosilicates, and modifiers tend to convert boron units from 3- to 4-coordination, in other words change the bonding around the boron from 3-oxygen to 4-oxygen, until the modifier concentration is greater than 50%. After this point, the cations will associate with either Si or B, creating NBOs[8]. In borosilicate systems, where sodium is the only added alkali, phase separation on the 5-20nm scale may occur due to large immiscibility regions[9]. In these systems with less sodium, the boron is more likely to be found in 3-coordination. This coordination causes the boron, and any attached sodium, to be more susceptible to leaching via acid[1]. Leaching is a term used to describe the release of material from the glass due to the environment. Leaching can occur in an aqueous atmospheres or when a glass is submerged in a solution.

Aluminum is considered an intermediate constituent in glass as it can be found as a network former or modifier. In aluminosilicate glasses, all of the aluminum is thought to be found in tetrahedral form (surrounded by 4 oxygen), as long as the ratio of alumina to modifying oxides is less than one. In forming these tetrahedral, the aluminum consumes oxygen introduced by the alkali and alkaline earth modifiers, preventing any NBOs from forming[8, 9].

Although not terribly well defined, aluminoborate glass structure is believed to prefer forming 4-coordinated aluminum species to 4-coordinated boron species. This leaves no oxygen left to form NBOs. Theoretically, if the ratio of alumina to alkaline earth modifiers is one to one, then there are no free oxygen available to convert boron units from 3- to 4-coordination, thus the boron anomaly will not occur[9].

From these systems, it is clear that the combination of network formers with oxide modifiers will control the concentration of NBO in the glass structure. Additionally, the choice of oxides is important for changing the chemical durability of the glasses[10]. Adding aluminum to a borosilicate glass will greatly increase the chemical durability by retaining alkali modifiers. These modifiers with their mono-valiancy, or +1 charge, are likely to be charge balancing 4-coordinated aluminum and this association is strong enough to prevent them from being leached from the glass. Adding modifiers such and calcium and magnesium improves chemical durability because the NBO will situate around the ions, tightening the network[1]. Zirconia is added to experimental nuclear waste glasses to simulate the insoluble oxides of the radionuclides[11].

The chemical durability with respect to radionuclide containment is one of the most important features a waste glass must posses. This means that over time the toxic waste will not be released from the glass into the surrounding environment. This durability depends on how the environment interacts with the glass in terms of alteration and leaching. Significant research has been done on the alteration mechanisms and the alteration rate of these glasses[4, 12-15]. When water is introduced to a silicate system hydration, hydrolysis and interdiffusion of ions and protons occur by means of the following reactions[16]:

$$\mathrm{SiOR} + \mathrm{H_2O} \rightarrow \mathrm{SiOH} + \mathrm{R^+} + \mathrm{OH^-}$$

$$\mathrm{SiO_2} + 2\mathrm{H_2O} \rightarrow \mathrm{H_4SiO_4}$$

This reaction increases the pH of the system through the release of hydroxyl groups. Silicon and modifiers are then expected to release from the system through the reaction with water[16]. In acidic environments a similar reaction should occur (with hydronium in place of water), again raising the pH and leaching network formers and modifiers out of

the glass. This release is related to the NBO in the structure, where an ion associated with NBO is more likely to be released than an ion associated with a structural unit. Finally, in basic conditions the following reactions are expected:

$$OH^- + \equiv Si - O - Si \equiv \rightarrow \equiv SiOH \pm OSi \equiv$$

$$-OSi \equiv + H_2O \rightarrow \equiv SiOH + OH^-$$

$$\equiv Si - O - Si \equiv + H_2O \rightarrow \equiv SiOH + \equiv SiOH$$

Here, the hydroxyl breaks Si-O-Si bonds to form Si-OH bonds. Leaching in basic conditions is expected to occur less than for acidic conditions due to these mechanisms. Nuclear waste containment glasses are tested in these acidic and basic mediums because the waste itself is either acidic or basic, thus, the effect of the waste itself on the glass is an important reaction.

Following the reactions in acidic conditions, a gel layer, typically composed of silica, can be formed. This gel layer can form when ions that have diffused out of the material are re-deposited on the surface of the glass. Extensive study has been done this gel layer[17] especially with regard to the protective properties it offers. Once the layer has formed, interdiffusion can no longer occur, meaning that glass formers, modifiers and added radionuclides would be contained. The formation of the gel depends on the corrosion conditions and the composition of the glass[17, 18].

Adding oxides to form NBOs is essential for opening glass structure and allowing the incorporation of radionuclides. However, adding these oxides means that the chemical durability will be compromised. The purpose of this study is to determine correlations between glass composition (with respect to NBO content), environmental conditions (acidic and basic) and chemical durability in terms glass alteration. To determine the correlation of these conditions, three glass compositions with different amounts of NBOs were chosen. From the amount of NBO in the glass, the protective properties can be predicted. Here, it would be expected that the glass with the most NBO in its structure would be the weakest and thus be the most susceptible to corrosion. In contrast, the glass with the least NBO should be the least susceptible to reaction and therefore will corrode the least.

II. EXPERIMENTAL PROCEDURE

A. Sample Preparation

Three glass compositions were chosen to achieve different ratios of glass modifiers (providing NBO) to network formers (providing network tetrahedron) using values found in table 1(a). Table 1(b) shows the chosen compositional ratios, along with theoretical ratios of NBO to tetrahedron and NBO to bridging oxygen (BO).

Three 150g batches of each composition were prepared using Na_2CO_3, $CaCO_3$, ZrO_2, Al_2O_3, B_2O_3 and SiO_2 powders. The calculated compositions in mol% and wt% of the oxides are displayed in table 2.

Larger raw material powders were ground using a mortar and pestle and sieved through 100 mesh (150μm) pans. The powders were combined and mixed for melting. Each composition was melted in an alumina crucible at 1300°C for 1 hour and poured onto a graphite slab. After cooling to solidification, each glass was transferred to an annealing oven where it was held at 570°C for 3-4 hours and then cooled to room temperature.

After cooling, the glass was broken and ground into powder using an agate mortar and pestle. The glass powders were sieved to 32-90μm and collected for ultrasonic cleaning in acetone (10-15 minutes, 19-25 times) until the supernatant was clear. Each sample was covered loosely with parafilm and dried in air. The mass and density of each glass was used to calculate specific surface area (SSA), assuming spherical particles (table 3).

B. Corrosion Methods

Solutions of pH 3 (±0.03) were prepared by adding HCL to DI water, and solutions of pH 9 (±0.01) were prepared by adding LiOH crystals to DI water. A pH meter calibrated at values of 4, 7, and 10, was used to measure the pH of all prepared solutions.

High-density polyethylene bottles were soaked in a nitric acid solution for 24 hours and DI water for 24 hours for cleaning. Each bottle was labeled using the sample identification (Glass 1, 2, or 3), pH of solution (3 or 9), and time of corrosion to be

performed in days (1, 3, 5, 10, 15). A SSA to volume ratio of $10m^{-1}$ was used to maintain consistency between the different glass surface areas and solution volumes (table 3). The bottles were placed in the oven for the specified number of days at 90°C. After the appropriate time period, the bottles were removed from the oven and 30ml of solution from each was filtered and collected for ICP analysis. The remaining solution was decanted and the power was collected, cleaned in DI water and isopropanol, and finally dried.

C. Materials Characterization

X-Ray Diffraction

X-ray diffraction (XRD) was performed with a Bruker D2 Phaser to confirm amorphous structures. Each powder was mixed with isopropanol and deposited onto the surface of a zero background holder. Measurements were taken using Cu $K_{\alpha 1}$ x-rays from 5-70°2θ, with a step size of 0.03 for 1 step/s. Jade XRD Pattern Processing, Identification, and Quantification software was used to compare the patterns against standard XRD patterns from the ICDD PDF-4+ 2012 database.

X-Ray Photoelectron Spectroscopy

X-ray photoelectron spectroscopy (XPS) was used to determine the change in composition (in terms of atomic percent, at%) of the surface by measuring the pre- and post-corrosion samples. XPS was performed using a PHI Quantera Scanning X-Ray Photoelectron Microprobe. Data was collected using monochromatic Al Kα x-rays. Survey scans were performed with a pass energy of 140eV and a step size of 0.025eV, and Os1, Si2p, Al2p, B1s, Zr3d, Ca2p, and Na1s peaks were detected. Tolerance for the peak position was ±0.3eV. Peak analysis was performed with MultiPak software, and used with relative sensitivity factors to determine atomic percentages within a ±0.1% tolerance. Calibration was based on the difference between the standard (284.60eV) and measured C1s peak.

Inductively Coupled Plasma Spectroscopy

Inductively Coupled Plasma Spectroscopy (ICP) was used to determine the concentration of ions in solution. Each sample was composed of 1mL corrosion solution and 9mL DI water to achieve a 1:10 dilution. A Perkin Elmer Optima 8000 ICP-OES Spectrometer was used for measurements. Samples of the pH 3 and pH 9 solutions were used to create a baseline for the results. The oxide concentration was normalized with respect to the original mol% concentration in the glass using the following formula:

$$C_{normalized} = \frac{C_{solution}}{C_{glass}}$$

where $C_{solution}$ is the concentration of ions in solution (converted from ppm to mol%) and C_{glass} is the oxide mol% in the original glass. This concentration was then used to normalize according to surface area using the following formula:

$$X_{normalized} = \frac{C_{normalized}}{SA * m}$$

where SA and m are the surface area and mass of the glass, respectively. By normalizing the data this way, the release of ions by all of the glasses can be compared.

Scanning Electron Microscopy

A FEI Quanta 200F Environmental Scanning Electron Microscope was used to image pre-corrosion and 15-day corrosion powders. All powders were mounted to studs using carbon tape, and coated with Au-Pd to minimize charging. Secondary and backscattered electrons were used to capture images at 500x, 5000x and 20000x magnification, with an accelerating potential of 10kV, and a spot size of 3.

III. RESULTS

A. *X-ray Diffraction*

XRD patterns of the unreacted powders for Glasses 1, 2, and 3 can be seen in figure 1(a). All glasses showed amorphous humps spanning 5-68°2θ, with additional small humps around 68-70°2θ. Patterns for the corroded samples for Glasses 1, 2, and 3 in pH 3 and pH 9 solutions can be seen in figure 1(b). All samples show amorphous humps over the entire range. No significant crystalline peaks were detected in pre- or post-corrosion patterns using Jade software.

B. *X-ray Photoelectron Spectroscopy*

The calculated at% composition of the glass powder surfaces in terms of Na, Ca, Zr, B, Al, Si, and O for pre-corrosion and 15-day corrosion can be found in table 4. The at% of sodium and boron decreases in all samples after 15 days in both solutions. Boron reaches 0.0 at% in all 15-day solutions. The amounts of calcium, aluminum and silicon increase, and zirconium remains the same in all samples.

XPS survey spectra of the powders after 10- and 15-day corrosion, at pH 3 and pH 9 can be seen in figures 2, 3 and 4 for Glasses 1, 2, and 3, respectively. These spectra show changes in peak intensity. The sodium peak (1071eV) for all three glasses is significantly diminished after 10 days. The calcium peak (350eV) observes significant increase in Glasses 2 and 3. The oxygen peak (531) in Glass 1 is significantly diminished after 15 days in pH 3, and in pH 9 it increases from 10 to 15 days. The oxygen in Glass 2 is reduced in both solutions and in Glass 3 it appears to increase in pH 3 and remain constant in pH 9. The remaining peaks appear relatively constant in the survey scan.

C. *Inductively Coupled Plasma Spectroscopy*

ICP analysis of Glasses 1, 2, and 3 in solutions pH 3 and pH 9 for up to 15-day corrosion can be seen in figure 5 for silicon, sodium, and boron. The baseline from the solutions was used to calibrate the data, which was then normalized and plotted on a logarithmic scale.

Overall, sodium was released more than silicon and boron. Silicon released most from Glass 3 and least from Glass 1, with intermediate release from Glass 2. Sodium released most from Glass 1 and in similar amounts from Glasses 2 and 3. Boron released significantly more from Glass 1 and in very similar amounts from Glasses 2 and 3. All samples show a general increasing logarithmic trend of release with respect to time, a faster initial rate that gradually decreases.

D. *Scanning Electron Microscopy*

Figure 6 shows SEM images for Glass 1 powders, captured from a combination of secondary and backscattered electrons, at 20000x magnification. Figures 6(a), 6(b), and 6(c) correspond to powders: pre-corrosion, after 15 days in a solution of pH 3, and after 15 days in a solution of pH 9. Images of the same designation for Glasses 2 and 3 can be found in figures 7 and 8 respectively, although images shown for Glass 3 were captured at 5000x.

Glass 1 showed the least change in surface morphology of any samples, no evidence of surface layer formation in either solution, but possible deposition in pH 9. Glasses 2 and 3 in both solutions showed evidence of precipitate deposition, while surface layer formation was only apparent those glasses in pH 3. In addition, a crack appears on the surface of Glass 2 in pH 3.

IV. DISCUSSION

Initial characterization

Characterization of the pre-corrosion powders using XRD was performed to determine if the powders were completely amorphous. The patterns in figure 1(a) show amorphous humps spanning 5-40°2θ, which include a descending tail from 40-67°2θ. Around 68°2θ, a small hump appears. Jade analysis software was used to check for potential peak identification within the small hump, however no significant peaks matched the patterns. The XRD patterns in figure 1(b), from the 15-day corroded glass powders, showed amorphous humps from around 5-40°2θ again, but with a slightly different shape. XRD is not used to identify glass structure, however the pre- and post-corrosion patterns differ enough that it can be concluded that the structure changed during corrosion. It is also worth noting that a systematic error of the XRD instrument can be seen in figure 1(b) as the vertical lines at the beginning of the measurement.

Evidence of leaching

The data from XPS indicates a change in the surface composition of all three glasses. Table 4 shows consistent concentrations of zirconium in all samples and conditions. This is consistent with the idea that zirconium acts as the insoluble waste component[11] and shows that all glasses were successful in contain the mock waste product. All three glasses show a decrease in at% for Na and B, with an increase in at% for Ca, Al, Si, and O. This indicates that Na and B were leached from the powder leaving a Ca, Al, and Si rich surface. The XPS spectra for all glasses show the Na1s peak (located around 1071eV) diminished after the 10-day corrosion, corresponding to the decrease in at% Na. The increase in the calcium peak is expected, as it will make up a large portion of the composition when other constituents are leached out. The changes in oxygen peaks could indicate deposition or a change in the bonding environment from NBO to BO or Bo to NBO.

Data from XPS and ICP correspond and show that leaching of ions from the glass surface into solution occurred during corrosion. ICP results show no significant leaching

of calcium or aluminum, and no leaching of zirconium, which corresponds with XPS analysis. Figure 5 shows normalized amounts of silicon, sodium, and boron in solution. All glasses in both pH solutions show an increasing trend of ions in solution with time, with a fast initial rate that gradually decreases over time, a trend described readily in previous studies[16, 19]. Generally, sodium leached the most, silicon leached the least, and boron was intermediate but closer to silicon amounts.

The ICP results for Glass 1 after 15-days in pH 3 were significantly different during the initial run (ppm values were several thousand as compared all other samples around several hundred), and were retested. The results from this run still deviate from expectations as noted by the decrease in all ions in solution. It is possibly that minimal deposition of the ions back onto the glass occurred, however significant deposition was not observed using SEM.

Figure 5(a) shows that Glass 1, which theoretically had no NBOs, has the least amount of silicon leached from the surface. This is expected, as stronger glasses should retain more network formers. Glass 3, which had the most NBOs/Tetrahedron, leached the most silicon. Because Glass 3 should be the weakest in terms of network strength, it is expected to leach the most silicon. It is also interesting to note that all glasses leached more silicon in the pH 9 solutions.

Sodium leached the most from Glass 1, and in comparable amounts from Glasses 2 and 3. It is not surprising that of all the ions, sodium was the most prevalent in solution because it is a modifier prone to leaching. However, it would be expected that the strong network of Glass 1 would retain these ions more than Glass 2 or 3. With the concept that sodium ions would be most stable in the structure with more aluminum, then it would be expected that Glass 1, with the smallest Al/Na ratio, would retain the most sodium. These results of ICP could indicate that the sodium is not surrounding the aluminum units, but instead the boron units. This would correspond to a sodium-boron rich phase.

Boron showed a similar trend to sodium, with Glass 1 leaching more than the others. It is interesting to note that the leaching of boron in Glass 1 was significantly higher than boron leaching of Glasses 2 and 3, both of which were closer than observed

for silicon or sodium. Perhaps the lack on NBOs in Glass 1 left the boron as 3-coordinated units in the structure. These Q_3 species would experience less network connectivity than Q_4 and would therefore be more susceptible to leaching.

Evidence of Surface Features

Following leaching, it is expected that the glass surface layer will be significantly changed and ideally, a silica gel layer would have formed, preventing further ion diffusion. SEM imaging allowed for qualitative visual analysis of the powder surfaces. Figures 6(a), 7(a), and 8(a) show Glasses 1, 2, and 3, respectively, before corrosion. There are no notable surface features on Glasses 1 or 2, and only evidence of grinding seen in hackle for Glass 3.

Figure 6(b) shows Glass 1 after 15 days in the pH 3 solution. The image does not show evidence of surface layer formation or precipitate deposition. Figure 6(c) shows Glass 1 after 15 days in the pH 9 solution, which shows again, no evidence of surface layer formation, but possible precipitate deposition. Overall, the effect of aqueous corrosion on Glass 1 appears to be minimal as compared to Glasses 2 and 3. This was the expectation, as Glass 1 theoretically contains no NBO, and should therefore be the most corrosion resistant.

Figures 7(b) and (c) show Glass 2 after 15 days in pH 3 and pH 9, respectively. Significant deposition can be seen after the pH 3 corrosion, where there is also surface layer formation occurring. A crack seen in the middle of the image could be the result of cracking of the surface layer with dehydration. It was postulated that the deposition could be due to the hydrochloric acid solution, however XRD did not show any crystalline peaks corresponding to chlorine. The same glass in pH=9 lacks the same significant surface layer formation, but does show features from pre-corrosion grinding. The appearance of a surface feature in the middle of the image could indicate some deposition has occurred, but it is not as significant as the deposition in figure 7(b).

Glass 3 after 15 days in pH 3 can be seen in figure 8(b). This image shows significant evidence of surface layer formation. There appears to be growth on the surface

of the powder as shown by the shelf-like feature seen near the bottom left of the image. Additionally, there appears to be pitting of the surface. This could be due to sodium-boron riches phases in the glass that have leached out as indicated by XPS and ICP analysis. There also appears to be some particle deposition on the surface. The same glass in pH 9 shows potential precipitate deposition, but lacks evidence of surface layer formation.

Clearly, glass composition and pH both effect corrosion of the glass. Glass 1 was the least affected by corrosion overall, while Glasses 2 and 3 showed significant evidence of surface layer formation and particle deposition in pH 3, but were less effected by pH 9 solutions. This result corresponds to the expected reactions in a basic medium.

V. CONCLUSIONS

These corrosion experiments show that pH and glass composition, in particular NBO concentration, significantly affect the release of silicon, sodium, and boron into solution. XPS and ICP analysis showed leaching of sodium and boron occurring in all glasses regardless of composition or pH. Additionally, ICP data indicates silicon was leached the most from Glass 3, the NBO rich glass, and least from Glass 1, the NBO lacking glass, showing a correlation between NBO concentration and leaching of the network formers. SEM and XPS indicate the presence of a sodium- and boron-depleted surface layer formation for Glasses 2 and 3 after reaction at pH 3, with no evidence of a surface layer forming in pH 9 solutions.

VI. FUTURE WORK

The next steps for this project are determining the glass structures and NBO abundance for each composition, as well as characterizing the developed surface features. In order to fully compare the result based on composition, it would be useful to learn more about the actual glass structures. Nuclear magnetic resonance spectroscopy with ^{29}Si, ^{27}Al, and ^{11}B magic-angle sample spinning techniques[20] would provide information about the bonding environments of the network formers and NBOs. Additionally, XPS high resolution scans of the O1s peak for pre- and post-corrosion powders would help identify the NBO concentration of each glass. XPS high resolution scans of silicon, aluminum and boron peaks would also shed light on the bonding environments. Raman and infrared spectroscopy on all powders would show structural changes in the glasses, hopefully indicating the formation of a silica gel layer. IR spectroscopy would also give relative NBO concentration, allowing for a comparison between compositions.

Further characterization of the surface features on Glasses 2 and 3 would allow greater understanding of the mechanisms of leaching and deposition. Energy dispersive spectroscopy would allow for a more focused measurement of the surface chemical composition, possibly confirming sodium-boron rich phases. Additionally, it may be worthwhile to consider XRD performed with smaller step size and longer step time, which would result in more intense peaks, helping to identify any crystalline deposition or minor phase separation of the glasses

If the experiment were repeated it would be valuable to measure the pH of the solutions during the corrosion experiments. This would help to track changes that occur due to leaching to better understand the alteration mechanisms and reactions. On the other hand, it may be valuable to change out solutions or buffer them during the corrosion to keep a consistent pH.

VII. APPENDIX

Table 1. Contribution of NBO (a) and resultant NBO/tetrahedron and NBO/BO for each glass composition (b).

	NBO/mol	Network Tetrahedron/mol
Na_2O	2	0
CaO	2	0
ZrO_2	0	0
Al_2O_3	-2	2
B_2O_3	-2	2
SiO_2	0	1

(a)

Glass	Modifier/ Network former	NBO/ Tetrahedron	NBO/ BO
1	0.95	0.000	0.000
2	1.25	0.091	0.044
3	1.50	0.170	0.080

(b)

Table 2. Compositions of Glasses 1, 2, and 3 in (a) mol% and (b) wt%.

	Glass 1	Glass 2	Glass 3
Na_2O	13.30	15.17	16.40
CaO	5.50	6.27	6.80
ZrO_2	1.50	1.50	1.50
Al_2O_3	4.00	3.47	3.12
B_2O_3	15.80	13.69	12.32
SiO_2	59.90	59.90	59.90

(a)

	Glass 1	Glass 2	Glass 3
Na_2O	12.83	14.73	15.99
CaO	4.80	5.51	6.00
ZrO_2	2.88	2.90	2.91
Al_2O_3	6.35	5.54	5.00
B_2O_3	17.12	14.93	13.49
SiO_2	56.02	56.39	56.61

(b)

Table 3. Calculated specific surface area for Glasses 1, 2, and 3 and solution volume satisfying a $10 m^{-1}$ ratio.

Glass	Specific Surface Area (m^2/g)	Solution Volume for 2 g Sample (mL)
1	1.2505E-03	250.1
2	1.2615E-03	252.3
3	1.2735E-03	254.7

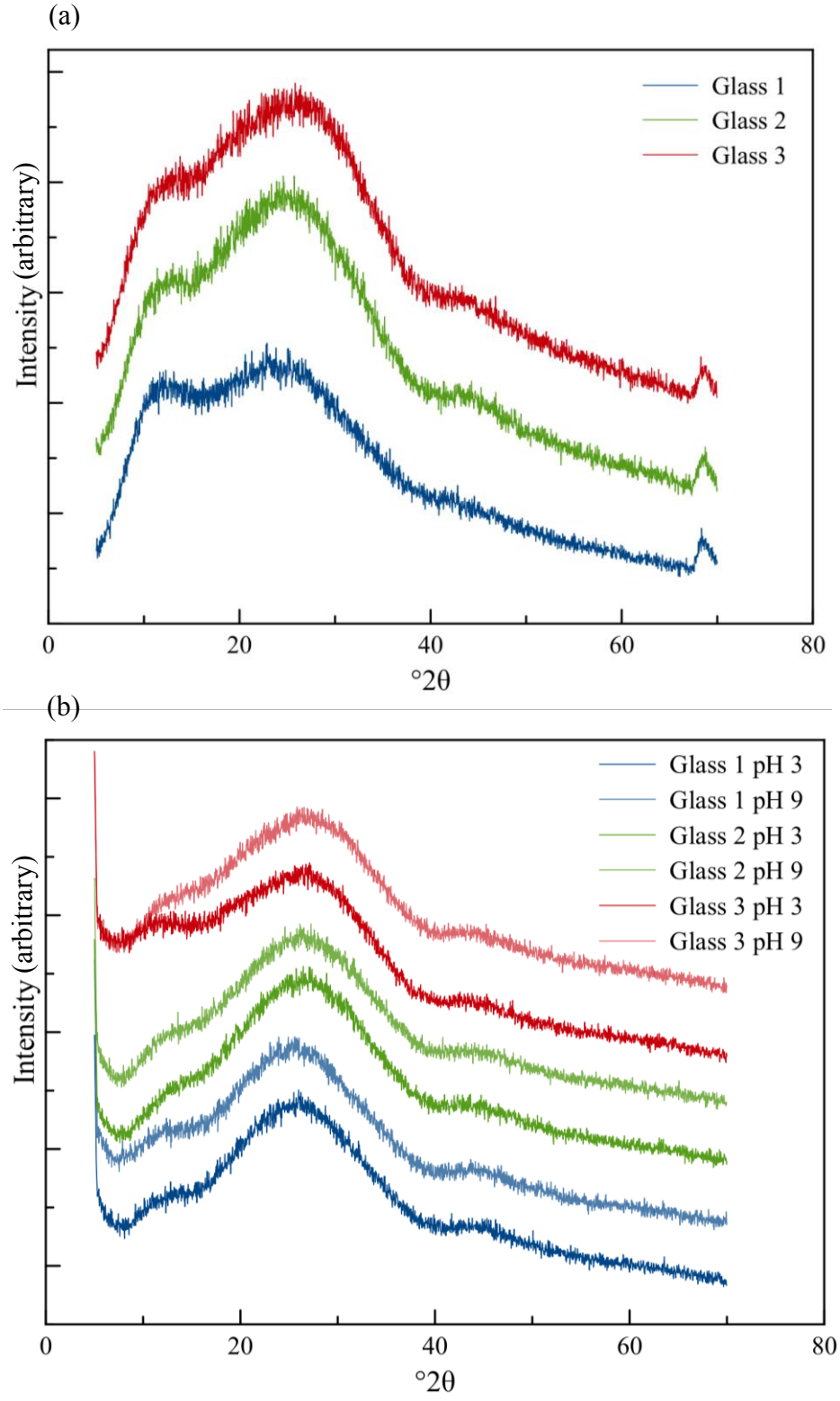

Figure 1. XRD patterns of glass powders (a) before and (b) after corrosion.

Table 4. Atomic compositions as determined by XPS of (a) Glass 1, (b) Glass 2, and (c) Glass 3, pre-corrosion and after 15-day corrosion.

	Pre-corrosion	pH=3	pH=9
Na	10.0	2.0	1.8
Ca	0.3	1.2	1.4
Zr	0.5	0.5	0.5
B	14.5	0.0	0.0
Al	2.3	5.0	5.9
Si	16.9	25.8	26.2
O	55.5	65.5	64.3

(a)

	Pre-corrosion	pH=3	pH=9
Na	9.5	0.8	0.9
Ca	0.3	1.9	1.5
Zr	0.5	0.5	0.5
B	10.7	0.0	0.0
Al	2.3	5.2	5.1
Si	18.7	26.1	26.9
O	58.0	65.5	65.2

(b)

	Pre-corrosion	pH=3	pH=9
Na	10.5	0.7	0.7
Ca	0.4	1.6	1.2
Zr	0.5	0.5	0.5
B	11.3	0.0	0.0
Al	2.1	4.8	5.6
Si	17.2	26.5	30.4
O	58.0	65.8	61.6

(c)

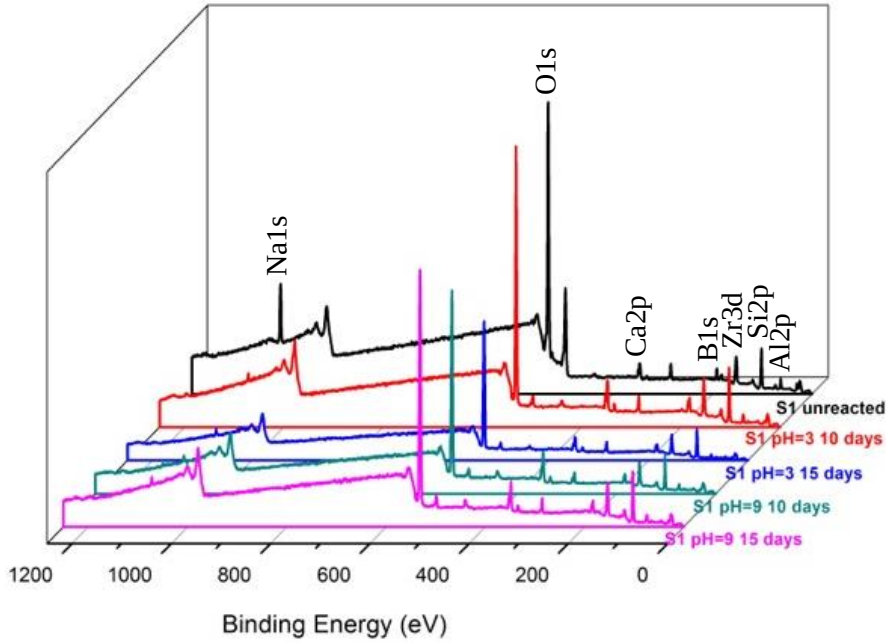

Figure 2. XPS spectra of Glass 1 after 10- and 15-day corrosion in pH=3 and pH=9 solutions.

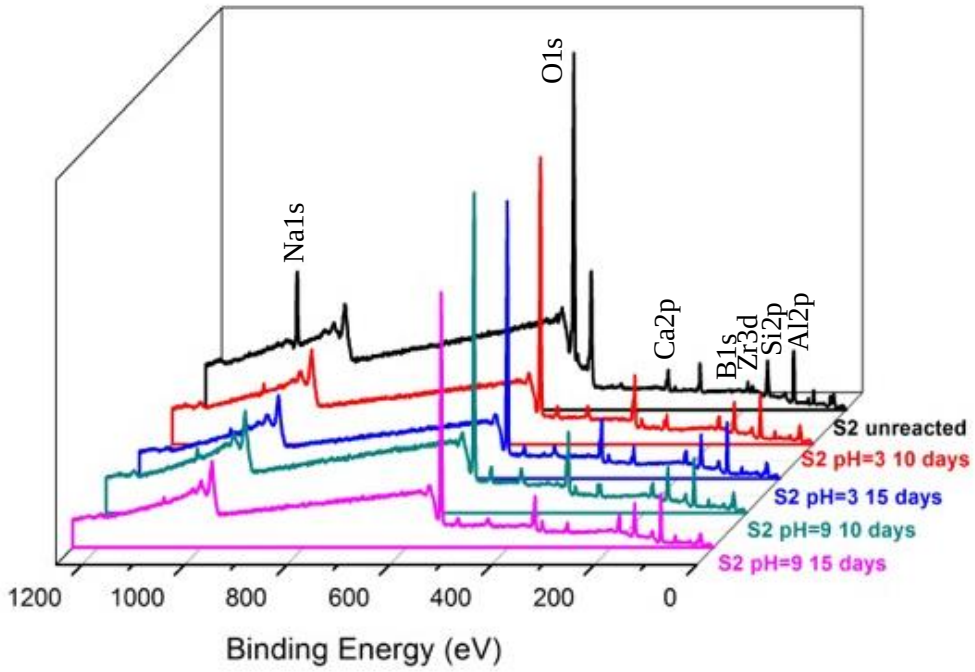

Figure 3. XPS spectra of Glass 2 after 10- and 15-day corrosion in pH=3 and pH=9 solutions.

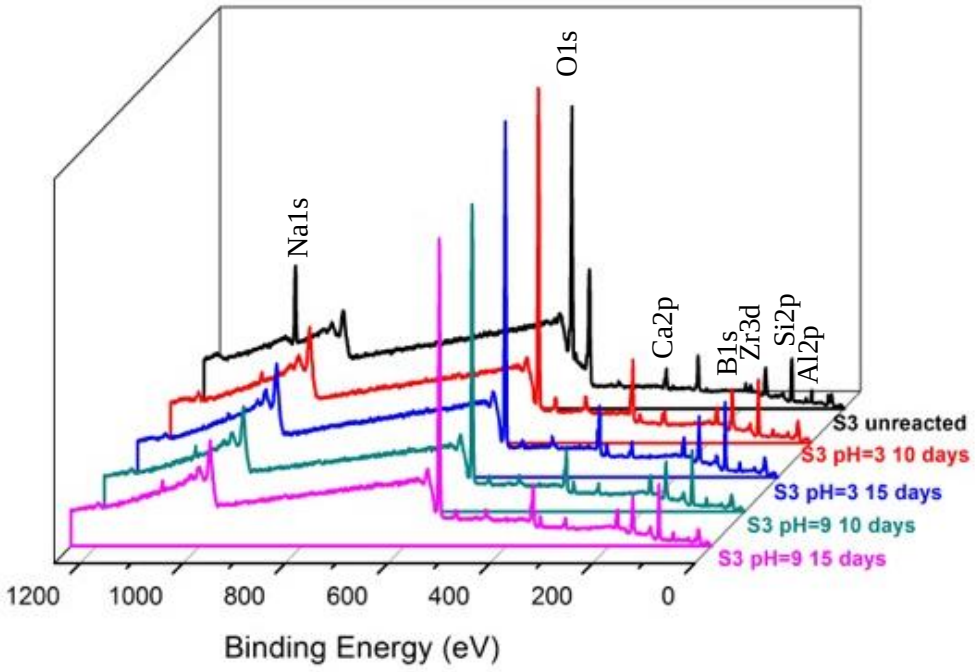

Figure 4. XPS spectra of Glass 3 after 10- and 15-day corrosion in pH=3 and pH=9 solutions.

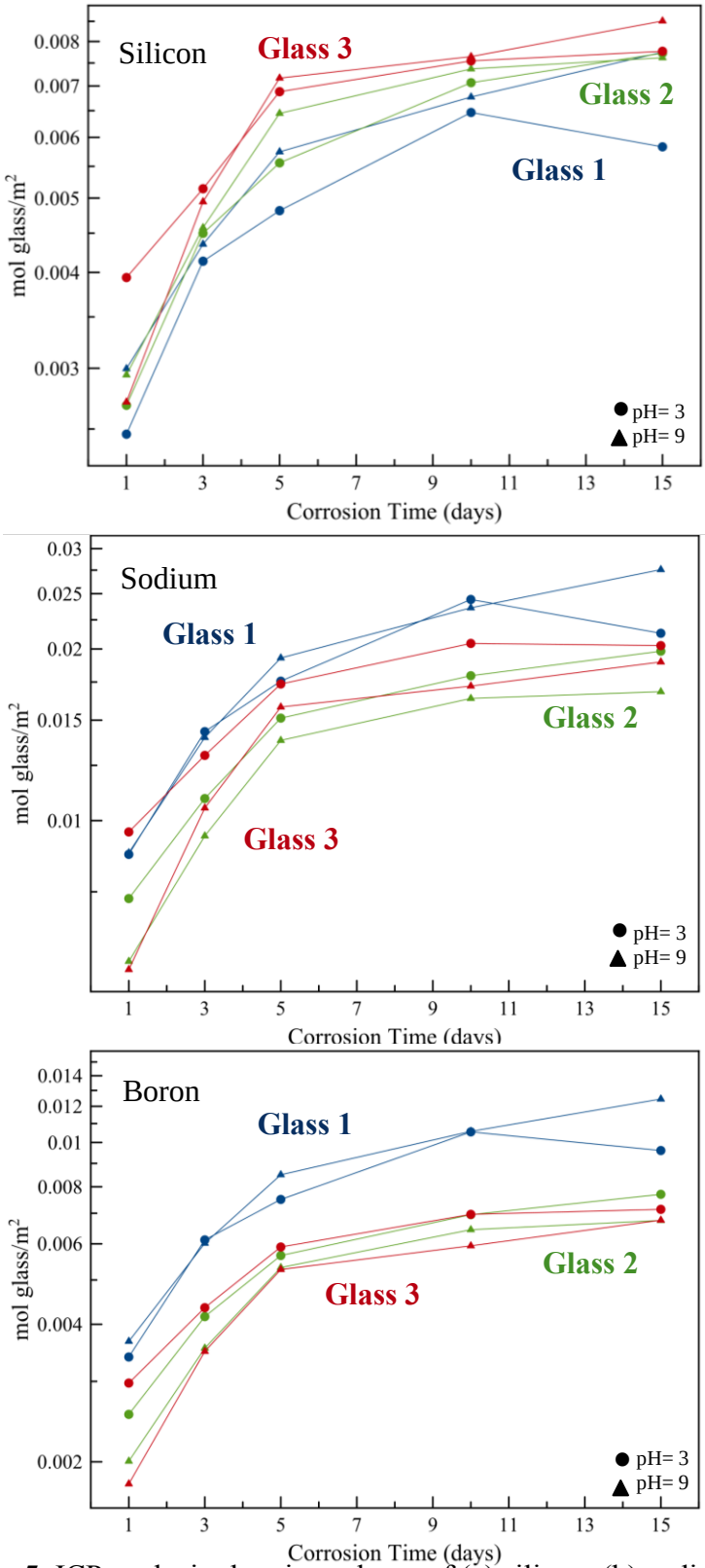

Figure 5. ICP analysis showing release of (a) silicon, (b) sodium, and (c) boron from Glasses 1, 2, and 3 into solutions (•) pH=3 and (▲) pH=9.

(a)

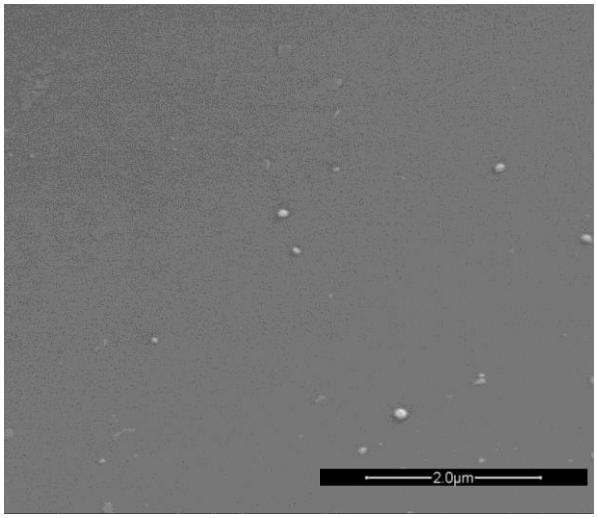

(b)

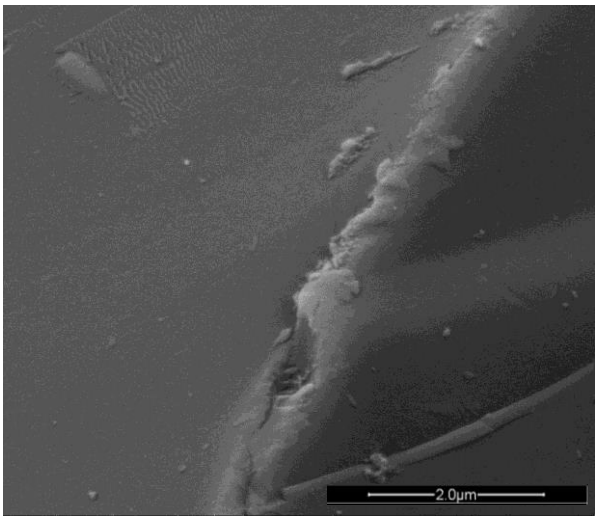

(c)

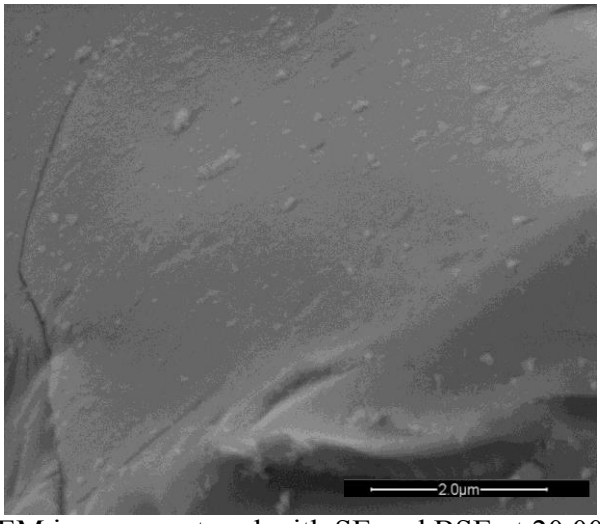

Figure 6. SEM images captured with SE and BSE at 20,000x magnification of Glass 1 (a) pre-corrosion, and after 15 days in (b) pH=3 and (c) pH=9

(a)

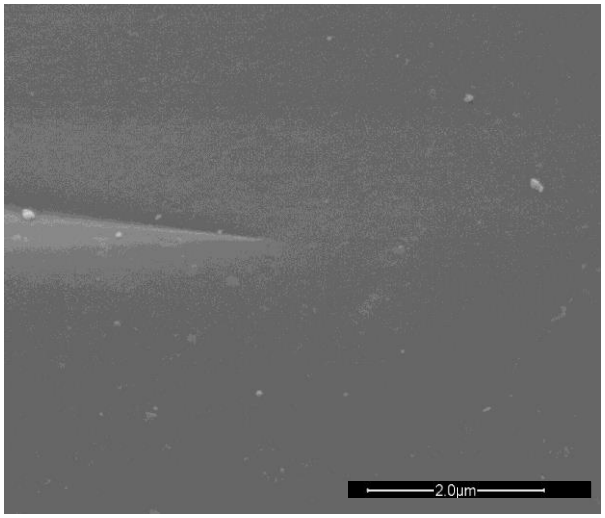

(b)

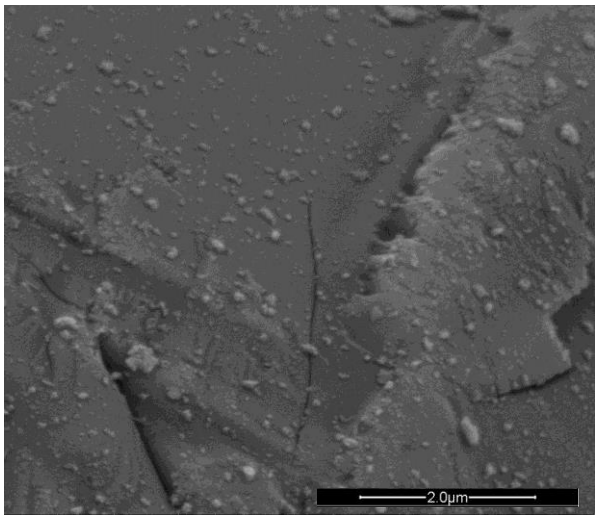

(c)

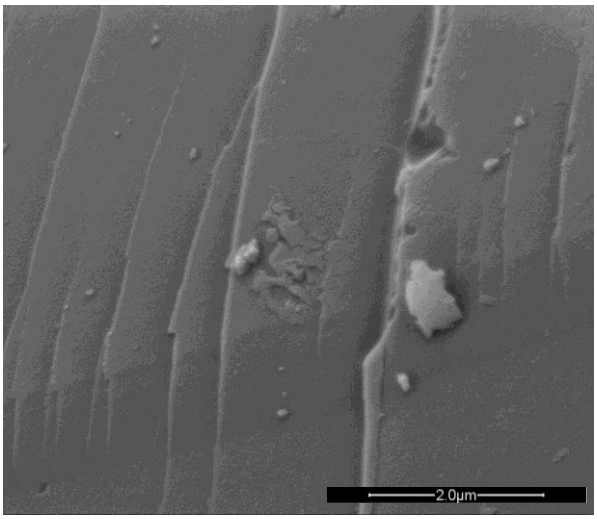

Figure 7. SEM images captured with SE and BSE at 20,000x magnification of Glass 2 (a) pre-corrosion, and after 15 days in (b) pH=3 and (c) pH=9

(a)

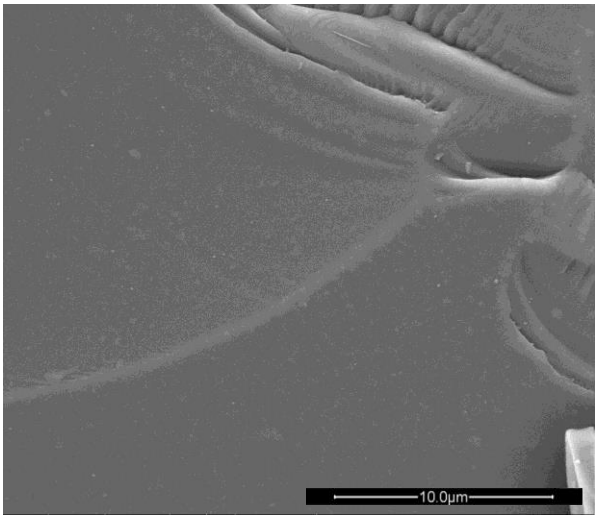

(b)

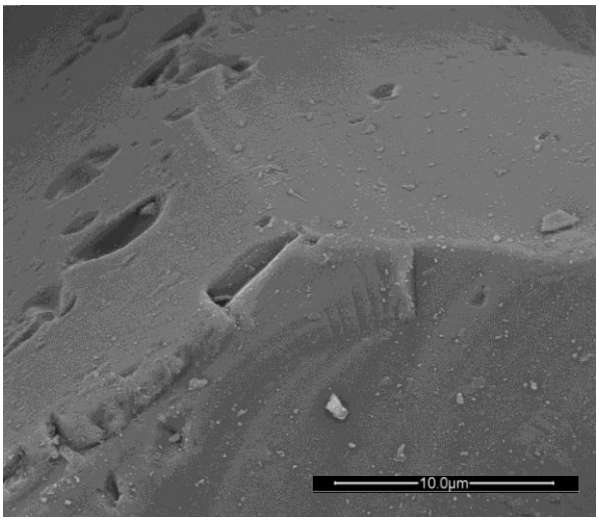

(c)

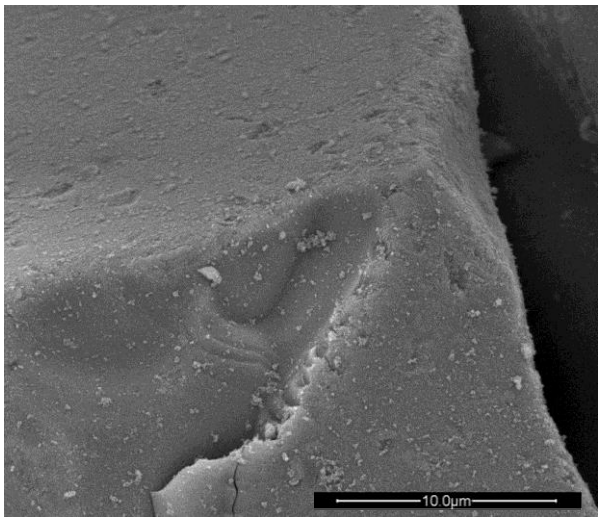

Figure 8. SEM images captured with SE and BSE at 5,000x magnification of Glass 3 (a) pre-corrosion, and after 15 days in (b) pH=3 and (c) pH=9

VII. REFERENCES

1. M. I. Ojovan and W. E. Lee, "An Introduction to Nuclear Waste Immobilisation," pp. 361. in. Elsevier, Oxford, 2014.

2. C. Poinssot and S. Gin, "Long-term Behavior Science: The cornerstone approach for reliably assessing the long-term performance of nuclear waste," *Journal of Nuclear Materials,* 420[1–3] 182-92 (2012).

3. J. Neeway, A. Abdelouas, B. Grambow, S. Schumacher, C. Martin, M. Kogawa, S. Utsunomiya, S. Gin, and P. Frugier, "Vapor hydration of SON68 glass from 90°C to 200°C: A kinetic study and corrosion products investigation," *Journal of Non-Crystalline Solids,* 358[21] 2894-905 (2012).

4. P. Frugier, C. Martin, I. Ribet, T. Advocat, and S. Gin, "The effect of composition on the leaching of three nuclear waste glasses: R7T7, AVM and VRZ," *Journal of Nuclear Materials,* 346[2–3] 194-207 (2005).

5. A. Verney-Carron, S. Gin, P. Frugier, and G. Libourel, "Long-term modeling of alteration-transport coupling: Application to a fractured Roman glass," *Geochimica et Cosmochimica Acta,* 74[8] 2291-315 (2010).

6. G. Libourel, A. Verney-Carron, A. Morlok, S. Gin, J. Sterpenich, A. Michelin, D. Neff, and P. Dillmann, "The use of natural and archeological analogues for understanding the long-term behavior of nuclear glasses," *Comptes Rendus Geoscience,* 343[2–3] 237-45 (2011).

7. A. Verney-Carron, S. Gin, and G. Libourel, "Archaeological analogs and the future of nuclear waste glass," *Journal of Nuclear Materials,* 406[3] 365-70 (2010).

8. A. K. Varshneya, "Fundamentals of Inorganic Glasses,*"* pp. 704 2nd ed. Society of Glass Technology, (2006).

9. J. E. Shelby, "Introduction to Glass and Technology,*"* pp. 291. Royal Society of Chemistry: UK, (2005).

10. S. Gin, X. Beaudoux, F. Angéli, C. Jégou, and N. Godon, "Effect of composition on the short-term and long-term dissolution rates of ten borosilicate glasses of increasing complexity from 3 to 30 oxides," *Journal of Non-Crystalline Solids,* 358[18–19] 2559-70 (2012).

11. C. Cailleteau, F. Angeli, F. Devreux, S. Gin, J. Jestin, P. Jollivet, and O. Spalla, "Insight into silicate-glass corrosion mechanisms," *Nature Materials,* 7[12] 978-83 (2008).

12. M. Debure, P. Frugier, L. De Windt, and S. Gin, "Dolomite effect on borosilicate glass alteration," *Applied Geochemistry,* 33[0] 237-51 (2013).

13. E. Burger, D. Rebiscoul, F. Bruguier, M. Jublot, J. E. Lartigue, and S. Gin, "Impact of iron on nuclear glass alteration in geological repository conditions: A multiscale approach," *Applied Geochemistry,* 31[0] 159-70 (2013).

14. A. Michelin, E. Burger, D. Rebiscoul, D. Neff, F. Bruguier, E. Drouet, P. Dillmann, and S. Gin, "Silicate Glass Alteration Enhanced by Iron: Origin and Long-Term Implications," *Environmental Science & Technology,* 47[2] 750-56 (2012).

15. E. Curti, J. L. Crovisier, G. Morvan, and A. M. Karpoff, "Long-term corrosion of two nuclear waste reference glasses (MW and SON68): A kinetic and mineral alteration study," *Applied Geochemistry,* 21[7] 1152-68 (2006).

16. E. Vernaz, S. Gin, C. Jégou, and I. Ribet, "Present understanding of R7T7 glass alteration kinetics and their impact on long-term behavior modeling," *Journal of Nuclear Materials,* 298[1–2] 27-36 (2001).

17. D. Rebiscoul, P. Frugier, S. Gin, and A. Ayral, "Protective properties and dissolution ability of the gel formed during nuclear glass alteration," *Journal of Nuclear Materials,* 342[1–3] 26-34 (2005).

18. B. M. J. Thien, N. Godon, A. Ballestero, S. Gin, and A. Ayral, "The dual effect of Mg on the long-term alteration rate of AVM nuclear waste glasses," *Journal of Nuclear Materials,* 427[1–3] 297-310 (2012).

19. D. Rebiscoul, A. Van der Lee, F. Rieutord, F. Né, O. Spalla, A. El-Mansouri, P. Frugier, A. Ayral, and S. Gin, "Morphological evolution of alteration layers formed during nuclear glass alteration: new evidence of a gel as a diffusive barrier," *Journal of Nuclear Materials,* 326[1] 9-18 (2004).

20. C. J. Simmons and O. H. El-Bayoumi, "Experimental techniques of glass science." American Ceramic Society, (1993).